Journal of the Australian Ceramic Society (2021) 57:287–293
https://doi.org/10.1007/s41779-020-00528-3

RESEARCH

$Ag_2O/GO/TiO_2$ composite nanoparticles: synthesis, characterization, and optical studies

Farzad Bayati[1] · Mohammad Kazem Mohammadi[2] · Reza Jalilzadeh Yengejeh[1] · Ali Akbar Babaei[1,3]

Received: 31 January 2020 / Revised: 23 September 2020 / Accepted: 16 October 2020 / Published online: 12 November 2020

Abstract

$Ag_2O/GO/TiO_2$ composite nanoparticles were synthesized via a two-stage route including wet chemical and sol-gel techniques. The phase regarding the composition and morphology of composite nanoparticles was characterized using X-ray diffraction (XRD), Fourier transfer infrared (FT-IR) spectroscopy, and field emission scanning electron microscopy (FESEM). The structural studies revealed the successful formation of 300-nm $Ag_2O/GO/TiO_2$ composite spheres self-assembled to 35-nm particle aggregates. UV-Vis diffuse reflectance spectroscopy (DRS) was utilized to investigate optical properties. The results indicated an absorption edge in the UV region with a band-gap equivalent to 3.2 eV for $Ag_2O/GO/TiO_2$ composite nanoparticles. The morphological features of the sample were investigated with a Zeiss (EM10C, Germany) transmission electron microscope (TEM) operating at 100 kV.

Keywords Silver oxide · Titanium dioxide · GO · Composite structures: nanoparticles

Introduction

Due to their considerable performances in electronics, photonics, solar cells, and environmental applications such as air and water purification, the development of nano-sized metal-oxide semiconductors has attracted increasing attention [1–7]. Since the observation of the photosensitization effect by Fujishima et al. in 1971 [1], titanium dioxide (TiO_2) semiconductors have been extensively studied because of their good biological and chemical stability, low cost, nontoxicity, and remarkable optical decomposition ability [8]. Titanium dioxide can be found in four forms of distinct polymorphs including anatase, rutile, brookite, and monoclinic phases [9]. TiO_2 nanostructures have been potential candidates for applications as pigments, optical filters, antireflection coatings, chemical sensors, sterilization materials, and catalysts [10]. A wide variety of techniques like the co-precipitation method [10], hydrothermal treatment [11], and sol-gel method [12] have been utilized for the synthesis of TiO_2 nanostructures. For example, Nagaraj et al. proposed a novel photon-induced method (PIM) to produce oxygen-rich TiO_2 with modified optical band-gap and high stability [13]. Abisharani et al. described the green synthesis of TiO_2 nanoparticles from titanium try chloride ($TiCl_3$) solution using the extract of *Cucurbita pepo* seeds [14]. In a study, nonaqueous reactions between titanium (IV) chloride and alcohols (benzyl alcohol or n-butanol) were employed for the synthesis of anatase TiO_2 particles, while aqueous media by acidic hydrolysis of titanium (IV) chloride were used for the preparation of rutile TiO_2 particles [15]. Ren et al. also formed a heterojunction between anatase TiO_2 nanosheets and anatase TiO_2 nanoparticles by a vapor-induced hydrothermal method followed by photothermocatalytic treatment to reach a significant improvement in photocatalytic activity [16].

It is believed that some key limiting factors, including the wide ban-gap, the fast photo-generated electron-hole recombination, and the low quantum efficiency, are confining practical applications of TiO_2 nanostructures to photocatalysis [17, 18]. In recent years, many researchers have focused on improving the photocatalytic performance of TiO_2 nanostructures by various methods such as doping with noble metals,

✉ Mohammad Kazem Mohammadi
mkmohamadi@gmail.com

[1] Department of Environmental Engineering, Ahvaz Branch, Islamic Azad University, Ahvaz, Iran

[2] Department of Chemistry, Ahvaz Branch, Islamic Azad University, Ahvaz, Iran

[3] Department of Environmental Health Engineering, School of Public Health, Ahvaz Jundishapur University of Medical Sciences, Ahvaz, Iran

non-metals, transition metals, and dyes [19]. It has been explored that coupling with metal-oxide semiconductors can be a suitable strategy for promoting photocatalytic performances of TiO_2 nanostructures [20]. In this way, Bandara et al. fabricated a new bilayer TiO_2/MgO nanoporous photocatalyst to minimize the charge recombination and achieve an enhanced photocatalytic activity [21]. Toloman et al. synthesized interface modified SnO_2-TiO_2 composite nanoparticles by a two-stage chemical precipitation process to investigate photocatalytic activity [22]. Hou et al. described the performance of $BiVO_4$@TiO_2 core-shell hybrid mesoporous nanofibers towards efficient visible light–driven photocatalytic hydrogen production. Gaurav et al. prepared ZnO:TiO_2 nanocomposites using the sol-gel method for photocatalyst application in the visible light [23]. The hybrid WO_3/TiO_2 photocatalysts were fabricated by Tahir et al. via the hydrothermal method for the degradation of methylene blue dye under visible light irradiation [24]. El-Sayed et al. also presented an investigation analysis on irradiated MgO-TiO_2 binary oxide synthesized by the sol-gel method [25].

Among various semiconductors, Ag_2O is a noble metal-oxide semiconductor with a band-gap ranging from 0.49 to 3.1 eV relevant to the quantum size effect [26, 27]. It has been reported that coupling n-type TiO_2 semiconductor with p-type Ag_2O leads to the formation of n-p heterojunctions resulting in separated photo-generated electron-hole pairs and inhibited charge carrier recombination [8]. To prepare nitrogen-doped TiO_2 thin films composed of ultrafine Ag_2O semiconductor nanoparticles with enhanced visible light absorption, Fang et al. utilized ion beam–assisted deposition [28]. Sadanandam et al. synthesized highly stabilized Ag_2O-loaded nanoTiO_2 using a hydrothermal-impregnation two-stage method for the photocatalytic production of hydrogen from glycerol:water mixtures under solar light irradiation [19]. Endo-Kimura et al. constructed Ag_2O/TiO_2 heterojunctions to examine the photocatalytic and antimicrobial properties for bacteria (*Escherichia coli*) and fungi (*Candida albicans* and *Penicillium chrysogenum*) [29].

It has been demonstrated that the structural benefits of binary heterostructured photocatalysts can be promoted through fabricating ternary graphene-based photocatalytic systems due to the high electron mobility (~ 15.000 m^2/V s) of charge carriers in graphene. Graphene has been reported to be a two-dimensional structure with excellent chemical stability, optical absorption, and mechanical strength resulting in improved charge separation and facilitated the formation of superoxide radicals [8, 30]. In this respect, Saleh et al. presented the fabrication of ternary Ag_2O/TiO_2/nanographene platelet composites using a microwave-assisted method for the degradation of organic dyes in aqueous solution [8]. Hou et al. demonstrated ultrasonic impregnation–assisted in situ photoreduction deposition synthesis of Ag/TiO_2/RGO ternary composites with a synergistic enhanced photocatalytic activity [30]. Liu et al. introduced integrating Z-scheme heterojunction into a novel Ag_2O@rGO@reduced TiO_2 photocatalyst with broadened light absorption and accelerated charge separation co-mediated highly efficient UV/visible/NIR light photocatalysis [31]. Herein, the synthesis of ternary Ag_2O/GO/TiO_2 composite nanoparticles has been reported by a two-stage route including wet chemical and sol-gel techniques and the characterization of Ag_2O/GO/TiO_2 nanoparticles using X-ray diffraction (XRD), Fourier transfer infrared (FT-IR) spectroscopy, field emission scanning electron microscopy (FESEM), and UV-Vis diffuse reflectance spectroscopy (DRS). These methods for the synthesis of this nanocomposite material were simple and versatile and the Ag_2O/GO/TiO_2 nanoparticles were stable in the synthesis processes. The existence of more available surface areas compared to that with simple structures resulted in more improved performances for potential applications such as photocatalysis. Also, these Ag_2O/GO/TiO_2 nanoparticles can be a useful catalyst for the synthesis of new heterocyclic organic compounds, drug delivery application, and drug discovery synthesis and also for removal degradation of organic dyes and antibiotics from wastewater.

Experimental section

Materials

Graphene oxide (GO) was purchased from Nano Altin Carbon. Other reagents and materials were obtained from Merck. All chemicals were at an analytical grade and utilized without further purification.

Synthesis of Ag_2O nanoparticles

A wet chemical technique was utilized to synthesize Ag_2O nanoparticles according to the literature [32]. In a typical synthesis process, 80 mL of a 0.005 M silver nitrate ($AgNO_3$) aqueous solution was heated at 60 °C. After that, 20 mL of a 0.025 M sodium hydroxide aqueous solution was added drop by drop to the prepared $AgNO_3$ solution under continuous magnetic stirring at 60 °C for 2 h. After cooling to room temperature, the formed precipitate was collected by a centrifuge with a speed of 3000 rpm, washed with ethanol several times, and dried at a constant temperature of 40 °C for 24 h.

Synthesis of Ag_2O/GO/TiO_2 composite nanoparticles

Ag_2O/GO/TiO_2 composite nanoparticles were synthesized through the sol-gel method according to a process reported by Xiao et al. [33] as follows: Firstly, 5 g of cetyltrimethylammonium bromide (CTAB) as the precursor of TiO_2 was added into 30 mL of ethanol and kept under continuous stirring. Secondly, 25 mL of a butyl titanate solution that was separately dissolved in 50 mL of absolute ethanol, added into the obtained

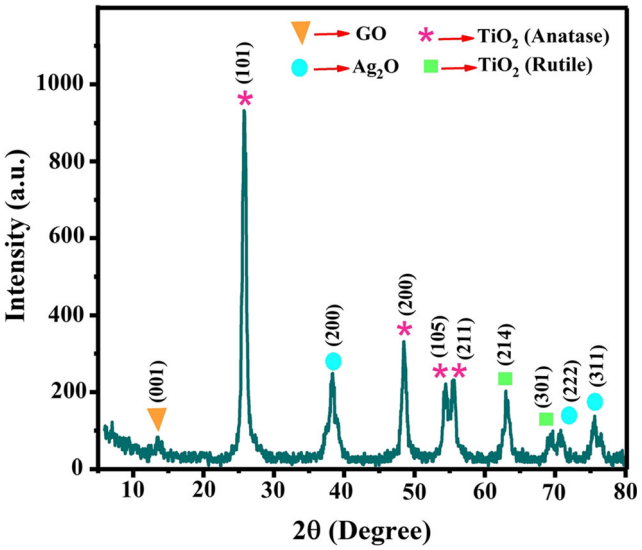

Fig. 1 XRD pattern of $Ag_2O/GO/TiO_2$ composite nanoparticles

CTAB solution at a rate of one drop every 3 s. Thirdly, a solution containing 7 mg of as-synthesized Ag_2O nanoparticles in 5 mL of absolute ethanol and another solution containing 20 mg of as-purchased graphene oxide in 10 mL of ethanol were prepared and after 1 h were slowly added to the above solution. The resultant mixture was stirred for 2 h to reach a titanium dioxide gel. The obtained product was finally dried at 65 °C for 12 h and calcined at 450 °C for 2 h.

Instrumental techniques

The crystalline phase of the as-synthesized sample was identified by X-ray diffraction (XRD) measurements by the means of a Ultima IV Multipurpose X-ray diffractometer equipped with Cu $K\alpha_1$ ($\lambda = 0.15406$ nm) radiation. Fourier transform infrared (FT-IR) spectrum was obtained using a Perkin Elmer BX-II spectrophotometer. Surface morphology was determined by a field emission scanning electron microscope (FESEM, Zeiss SIGMA VP-500) equipped with side detectors including energy-dispersive X-ray spectroscopy (EDS) and high-resolution elemental mapping to examine elemental compositions. Ultraviolet-visible diffuse reflectance spectra (DRS) were recorded on a scan UV-Vis spectrophotometer (Avaspec-2048-TEC). The band-gap energy was estimated according to the Tauc method. The morphological features of the sample were investigated with a Zeiss (EM10C, Germany) transmission electron microscope (TEM) operating at 100 kV.

Results and discussions

Structural studies

Phase compositions of as-synthesized nanoparticles were identified using the X-ray diffraction (XRD) technique. Figure 1 displays the XRD pattern of $Ag_2O/GO/TiO_2$ composite nanoparticles. The XRD pattern of the composite nanoparticles exhibits four distinct peaks at 25.76°, 48.49°, 54.39°, and 55.53° corresponding to (101), (200), (105), and (211) crystal planes of anatase TiO_2 crystalline structure, respectively (JCPDS No. 00-021-1272). Two diffraction peaks are also found at 62.98° and 69.29°, which can be assigned to (214) and (301) planes of the TiO_2 rutile phase, respectively (JCPDS card No. 00-021-1276). The formation of Ag_2O structures is confirmed by arising characteristic peaks at 38.30°, 70.76°, and 75.55° relevant to (200), (222), and (311) Bragg planes, respectively (JCPDS No. 01-072-2108). As shown in Fig. 1, the presence of graphene sheets is justified by appearing a characteristic peak at 13.45° that can be indexed to carbon structures as presented in JCPDS Card No. 01-089-8491. It is well known that the existence of GO in semiconductor composite structures compared to other carbon materials can improve the transitional performance of charge carriers relevant to high-temperature thermal effects [33].

The surface chemical composition of the as-synthesized sample was investigated by FT-IR spectroscopy. Figure 2 shows the FT-IR pattern of $Ag_2O/GO/TiO_2$ composite nanoparticles in the range of 450–4000 cm^{-1}. It can be seen in Fig. 2 that, due to Ti-O stretching in TiO_2 lattice, the absorption band appears at 716.64 cm^{-1} [34]. The characteristic band at 2331.95 cm^{-1} is ascribed to the stretching modes of carboxyl (C=O) groups [14]. The band observed at 2828.11 cm^{-1} also corresponds to the C-H stretching frequency [34].

The surface morphology of the as-synthesized sample was observed using FESEM micrographs. FESEM images of $Ag_2O/GO/TiO_2$ composite nanoparticles in two different magnifications along with the corresponding histograms of particle size have been illustrated in Fig. 3. The FESEM image shown in Fig. 3a indicates a relatively uniform distribution from spherical-like particles with an average diameter of about 300 nm (Fig. 3c). It can be seen in Fig. 3b that the obtained

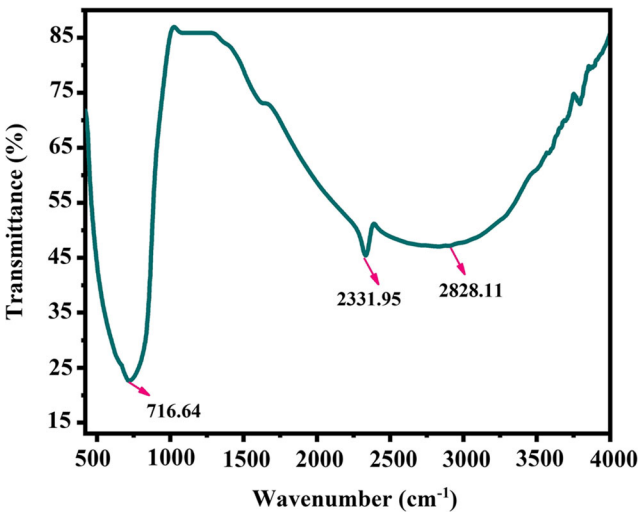

Fig. 2 FT-IR pattern of $Ag_2O/GO/TiO_2$ composite nanoparticles

spherical structures consist of numerous small nanoparticles with an average size of about 35 nm (Fig. 3d). Such a formed architecture revealed more available surface areas compared to that with simple spherical structures resulting in more improved performances for potential applications such as photocatalysis.

FESEM-EDS mapping was carried out to verify the surface element dispersion states of the as-synthesized sample. Figure 4 presents the results obtained from the FESEM-EDS mapping of $Ag_2O/GO/TiO_2$ composite nanoparticles. Figure 4b–e demonstrate the presence and uniform distribution of Ti, O, C, and Ag elements in the selected surface area of the as-synthesized sample (Fig. 4a), offering visual evidence for the successful formation of $Ag_2O/GO/TiO_2$ composite nanoparticles. EDS spectrum recorded for $Ag_2O/GO/TiO_2$ sample is also plotted as an inset in Fig. 4a, indicating the existence of Ti, O, C, and Ag with atom percentages of 50.3%, 23.1%, 6.3%, and 20.3% in $Ag_2O/GO/TiO_2$ composite structure, respectively.

The morphological features of the sample were investigated with a Zeiss (EM10C, Germany) transmission electron microscope (TEM) operating at 100 kV. These images were prepared as follows: The dilute aqueous solution of the sample was sonicated for 15 min. Then, a portion of the sample (20 μL) was dropped onto holey carbon film on copper grid 300 mesh (EMS, USA) and dried thoroughly at room temperature.

For the closer look of synthesized microstructures, the transmission electron microscope (TEM) was used. Transmission electron microscope image of $Ag_2O/GO/TiO_2$ is shown in Fig. 5. TEM image of $Ag_2O/GO/TiO_2$ is observed with 50 nm to 300 nm magnification. According to the figure, it can be said that the particles have irregular geometric shapes.

Optical studies

Optical characteristics of the as-synthesized sample were studied using UV-Vis diffuse reflectance spectra (DRS). Figure 5a demonstrates a UV-Vis absorption spectrum of $Ag_2O/GO/TiO_2$ composite nanoparticles in a wavelength range of 200–800 nm. It can be seen in Fig. 5a that $Ag_2O/GO/TiO_2$ composite nanoparticles exhibit a strong light absorption ability in the UV region with a steep edge towards the visible region. The absorption edge of $Ag_2O/GO/TiO_2$ composite nanoparticles can be precisely identified by estimating optical band-gap energy. The information on the band-gap energy (E_g) can be obtained using the Kubelka-Munk theory as follows [35, 36]:

$$(ahv) = A\left(hv - E_g\right)^{1/2} \quad (1)$$

where α presents the absorption coefficient, h is Planck's constant, ν is the light frequency, and A is the proportionality

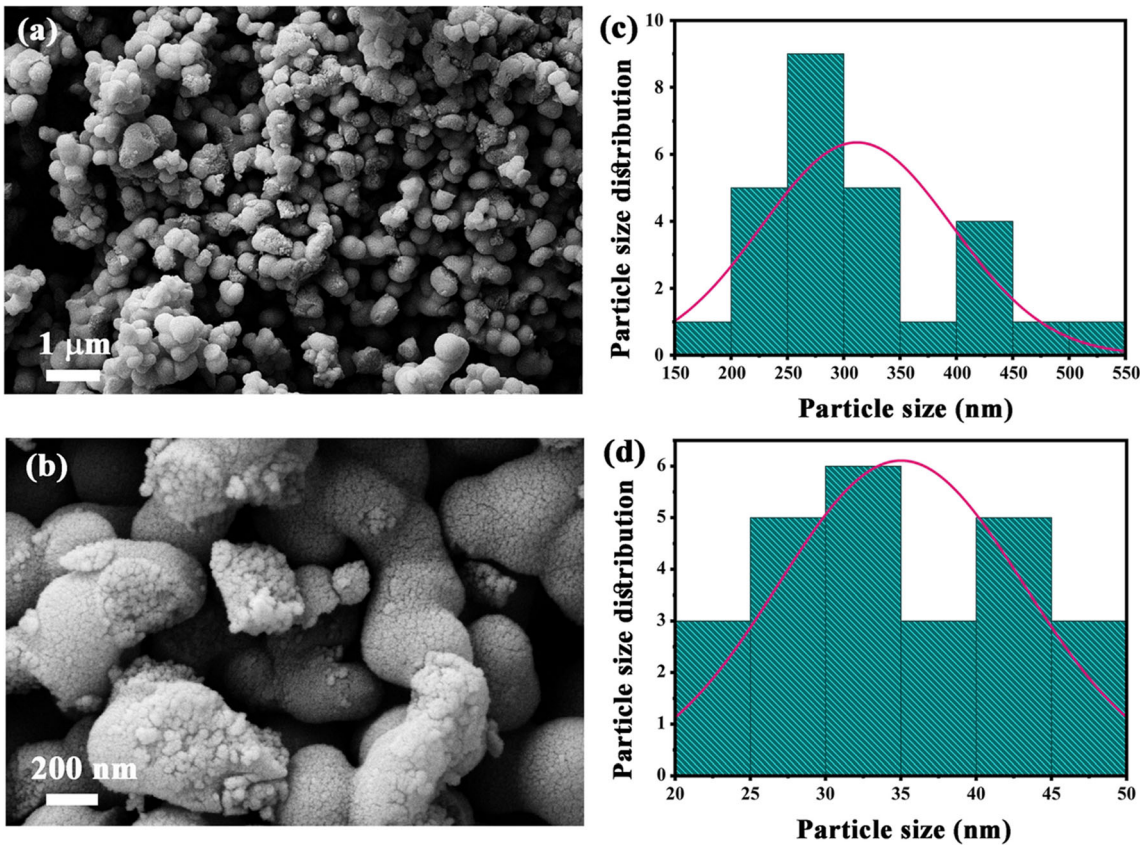

Fig. 3 **a**, **b** Typical FESEM images and **c**, **d** the corresponding histograms of particle size for $Ag_2O/GO/TiO_2$ composite nanoparticles

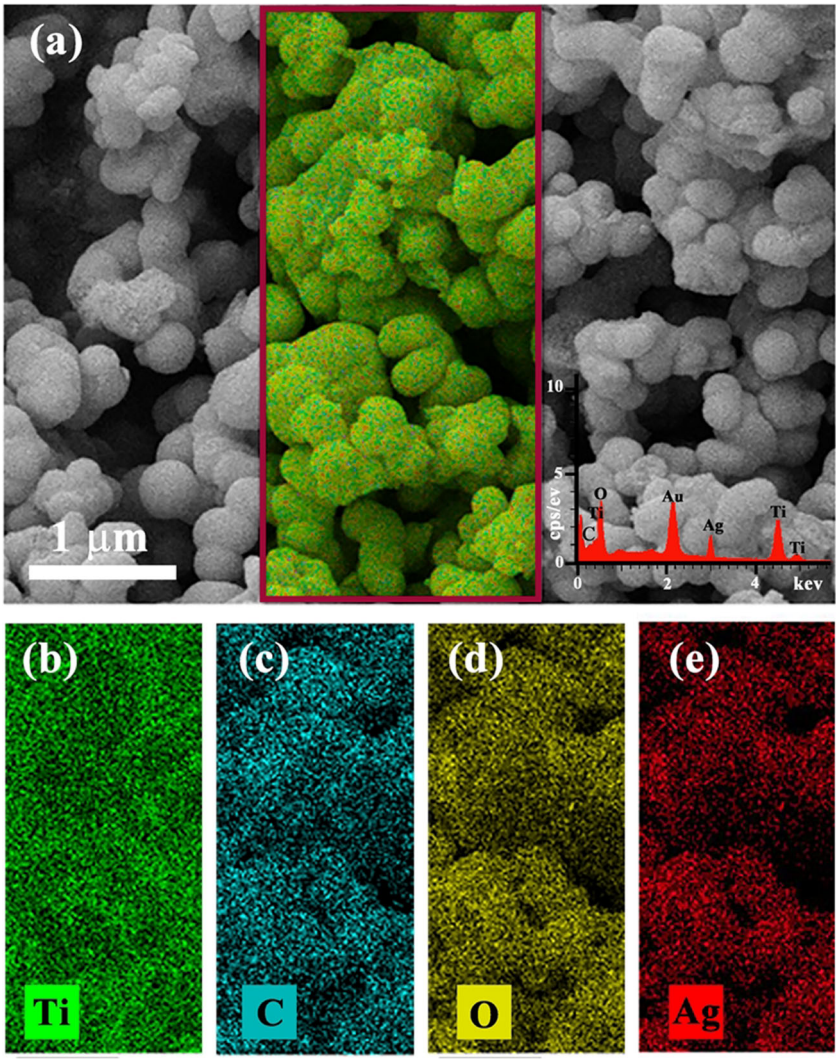

Fig. 4 **a** FESEM image; inset: corresponding EDS spectrum. **b**–**e** EDS mappings of $Ag_2O/GO/TiO_2$ composite nanoparticles

constant. According to the Tauc method, the numerical value of the band-gap energy is calculated by plotting $(ahv)^2$ against photon energy ($h\nu$) and then obtaining the intercept of the tangent to $h\nu$-axis. As given in Fig. 5b, the band-gap energy for $Ag_2O/GO/TiO_2$ composite nanoparticles is estimated to be about 3.2 eV. The optical absorption edge (λ_{max}) for $Ag_2O/$

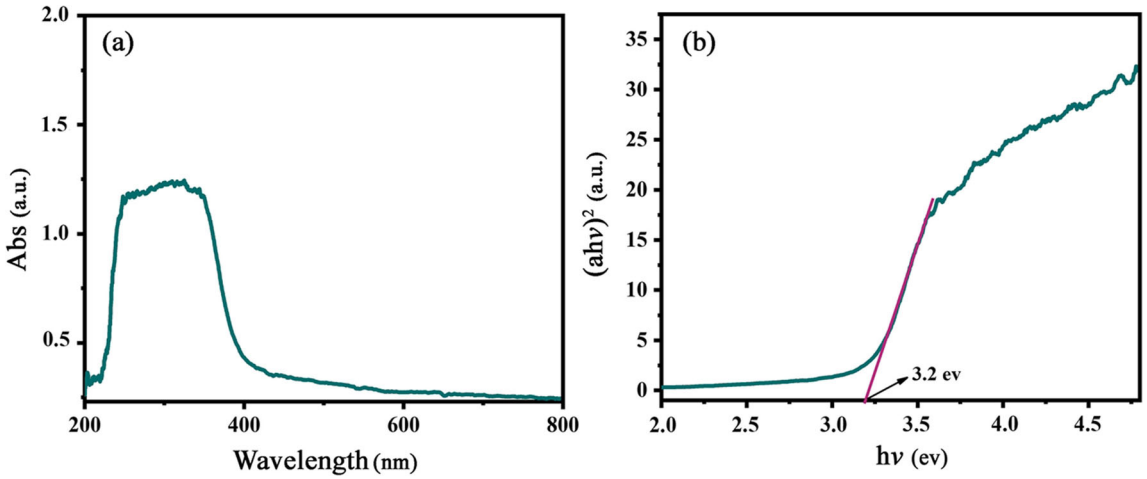

Fig. 5 **a** DRS spectrum and **b** the corresponding Tauc plot for $Ag_2O/GO/TiO_2$ composite nanoparticles

GO/TiO_2 composite nanoparticles can be also calculated as [37]:

$$\lambda_{max}(nm) = E_g(ev)/1240 \quad (2)$$

Therefore, an absorption edge of about 387 nm is calculated for as-synthesized $Ag_2O/GO/TiO_2$ composite nanoparticles. The obtained optical results indicate a UV-light-active material that can be used in possible applications benefiting from the advantages of the presence of UV light photons.

Conclusion

$Ag_2O/GO/TiO_2$ composite nanoparticles were successfully synthesized via a two-step process. The formation and composition of composite structures were investigated by the XRD, FT-IR, and FESEM methods. The structural studies demonstrated the fabrication of spherical structures with an average diameter of about 300 nm composed of nanoparticles with an average size of about 35 nm. The optical studies were also performed by UV-Vis diffuse reflectance spectroscopy and indicated an absorption edge in the UV region with a band-gap energy of about 3.2 eV. In conclusion, we found the versatile and simple method for the synthesis of new $Ag_2O/GO/TiO_2$ composite nanoparticles with the doped nanostructured Ag_2O and TiO_2 on the graphene surface that could the best candidate for future work in the wastewater treatment and synthesis of new organometallic compounds.

Supplementary Information The online version contains supplementary material available at https://doi.org/10.1007/s41779-020-00528-3.

Acknowledgments This work was partially supported by the Ahvaz Branch of Islamic Azad University and the authors would like to thank the Research Council for their generous support of this work.

References

1. Fujishima, A., Honda, K.: Electrochemical photolysis of water at a semiconductor electrode. Nature. **238**, 37 (1972)
2. Subramanian, V., Wolf, E., Kamat, P.V.: Semiconductor- metal composite nanostructures. To what extent do metal nanoparticles improve the photocatalytic activity of TiO2 films? J. Phys. Chem. B. **105**, 11439–11446 (2001)
3. S.U.M. Khan, M. Al-Shahry, W.B. Ingler, Efficient photochemical water splitting by a chemically modified n-TiO2, Science (80-.). 297 (2002) 2243–2245
4. Yu, J.C., Yu, J., Ho, W., Jiang, Z., Zhang, L.: Effects of F-doping on the photocatalytic activity and microstructures of nanocrystalline TiO2 powders. Chem Mater. **14**, 3808–3816 (2002)
5. R. Asahi, T. Morikawa, T. Ohwaki, K. Aoki, Y. Taga, Visible-light photocatalysis in nitrogen-doped titanium oxides, Science (80-.). 293 (2001) 269–271
6. Sakthivel, S., Kisch, H.: Photocatalytic and photoelectrochemical properties of nitrogen-doped titanium dioxide. ChemPhysChem. **4**, 487–490 (2003)
7. Burda, C., Lou, Y., Chen, X., Samia, A.C.S., Stout, J., Gole, J.L.: Enhanced nitrogen doping in TiO2 nanoparticles. Nano Lett. **3**, 1049–1051 (2003)
8. Saleh, R., Taufik, A., Prakoso, S.P.: Fabrication of Ag2O/TiO2 composites on nanographene platelets for the removal of organic pollutants: influence of oxidants and inorganic anions. Appl Surf Sci. **480**, 697–708 (2019)
9. Chenchana, A., Nemamcha, A., Moumeni, H., Rodríguez, J.M.D., Araña, J., Navío, J.A., Díaz, O.G., Melián, E.P.: Photodegradation of 2, 4-dichlorophenoxyacetic acid over TiO2 (B)/anatase nanobelts and Au-TiO2 (B)/anatase nanobelts. Appl Surf Sci. **467**, 1076–1087 (2019)
10. Viana, M.M., Soares, V.F., Mohallem, N.D.S.: Synthesis, and characterization of TiO2 nanoparticles. Ceram Int. **36**, 2047–2053 (2010)
11. Mathew, S., Kumar Prasad, A., Benoy, T., Rakesh, P.P., Hari, M., Libish, T.M., Radhakrishnan, P., Nampoori, V.P.N., Vallabhan, C.P.G.: UV-visible photoluminescence of TiO 2 nanoparticles prepared by hydrothermal method. J Fluoresc. **22**, 1563–1569 (2012)
12. Guang, M., Xia, Y., Wang, D., Zeng, X.-F., Wang, J.-X., Chen, J.-F.: Controllable synthesis of transparent dispersions of monodisperse anatase-TiO2 nanoparticles and nanorods. Mater Chem Phys. **224**, 100–106 (2019)
13. Nagaraj, G., Irudayaraj, A., Josephine, R.L.: Tuning the optical band gap of pure TiO2 via the photon-induced method. Optik (Stuttg). **179**, 889–894 (2019)
14. Abisharani, J.M., Devikala, S., Kumar, R.D., Arthanareeswari, M., Kamaraj, P.: Green synthesis of TiO2 nanoparticles using Cucurbita pepo seeds extract. Mater Today Proc. **14**, 302–307 (2019)
15. Abazovi, N.D., Omor, M.I., Anin, M.D.D., Jovanovi, D.J., Ahrenkiel, S.P., Nedeljkovi, J.M.: Photoluminescence of anatase and rutile TiO2 particles. J. Phys. Chem. B. **110**, 25366–25370 (2006)
16. Ren, L., Li, Y., Mao, M., Lan, L., Lao, X., Zhao, X.: Significant improvement in photocatalytic activity by forming homojunction between anatase TiO2 nanosheets and anatase TiO2 nanoparticles. Appl Surf Sci. (2019)
17. Lv, K., Fang, S., Si, L., Xia, Y., Ho, W., Li, M.: Fabrication of TiO2 nanorod assembly grafted rGO (rGO@ TiO2-NR) hybridized flake-like photocatalyst. Appl Surf Sci. **391**, 218–227 (2017)
18. Qiu, P., Sun, X., Lai, Y., Gao, P., Chen, C., Ge, L.: N-doped TiO2@ TiO2 visible light active film with stable and efficient photocathodic protection performance. J Electroanal Chem. **844**, 91–98 (2019)
19. Sadanandam, G., Valluri, D.K., Scurrell, M.S.: Highly stabilized Ag2O-loaded nano TiO2 for hydrogen production from glycerol: water mixtures under solar light irradiation. Int J Hydrog Energy. **42**, 807–820 (2017)
20. Yang, X., Wang, Y., Wang, Z., Lv, X., Jia, H., Kong, J., Yu, M.: Preparation of CdS/TiO2 nanotube arrays and the enhanced photocatalytic property. Ceram Int. **42**, 7192–7202 (2016)
21. Bandara, J., Hadapangoda, C.C., Jayasekera, W.G.: TiO2/MgO composite photocatalyst: the role of MgO in photoinduced charge carrier separation. Appl Catal B Environ. **50**, 83–88 (2004)
22. Toloman, D., Pana, O., Stefan, M., Popa, A., Leostean, C., Macavei, S., Silipas, D., Perhaita, I., Lazar, M.D., Barbu-Tudoran, L.: Photocatalytic activity of SnO 2 -TiO 2 composite nanoparticles modified with PVP. J Colloid Interface Sci. **542**, 296–307 (2019). https://doi.org/10.1016/j.jcis.2019.02.026

23. Upadhyay, G.K., Rajput, J.K., Pathak, T.K., Kumar, V., Purohit, L.P.: Synthesis of ZnO: TiO2 nanocomposites for photocatalyst application in visible light. Vacuum. **160**, 154–163 (2019)
24. Tahir, M.B., Farman, S., Rafique, M., Shakil, M., Khan, M.I., Ijaz, M., Mubeen, I., Ashraf, M., Nadeem Riaz, K.: Photocatalytic performance of hybrid WO3/TiO2 nanomaterials for the degradation of methylene blue under visible light irradiation. Int J Environ Anal Chem. 1–13 (2019)
25. El-Sayed, S.M., Amer, M.A., Meaz, T.M., Deghiedy, N.M., El-Shershaby, H.A.: Investigational analysis on irradiated MgO-TiO2 binary oxide. Mater Res Express. **5**, 56508 (2018)
26. Varkey, A.J., Fort, A.F.: Some optical properties of silver peroxide (AgO) and silver oxide (Ag2O) films produced by chemical-bath deposition. Sol Energy Mater Sol Cells. **29**, 253–259 (1993)
27. Kudryashov, D.A., Grushevskaya, S.N., Vvedenskii, A.V.: Determining some structure-sensitive characteristics of nano-sized anodic Ag (I) oxide from photopotential spectroscopy. Prot. Met. **43**, 591–599 (2007)
28. Fang, F., Li, Q., Shang, J.K.: Enhanced visible-light absorption from Ag2O nanoparticles in nitrogen-doped TiO2 thin films. Surf Coatings Technol. **205**, 2919–2923 (2011). https://doi.org/10.1016/j.surfcoat.2010.10.068
29. Endo-Kimura, M., Janczarek, M., Bielan, Z., Zhang, D., Wang, K., Markowska-Szczupak, A., Kowalska, E.: Photocatalytic and antimicrobial properties of Ag2O/TiO2 heterojunction. ChemEngineering. **3**, 3 (2019). https://doi.org/10.3390/chemengineering3010003
30. Hou, Y., Pu, S., Shi, Q., Mandal, S., Ma, H., Xue, S., Cai, G., Bai, Y.: Ultrasonic impregnation assisted in-situ photoreduction deposition synthesis of Ag/TiO2/rGO ternary composites with synergistic enhanced photocatalytic activity. J Taiwan Inst Chem Eng. **104**, 139–150 (2019). https://doi.org/10.1016/j.jtice.2019.08.023
31. Liu, X., Wang, Z., Wu, Y., Liang, Z., Guo, Y., Xue, Y., Tian, J., Cui, H.: Integrating the Z-scheme heterojunction into a novel Ag 2 O@rGO@reduced TiO 2 photocatalyst: broadened light absorption and accelerated charge separation co-mediated highly efficient UV/visible/NIR light photocatalysis. J Colloid Interface Sci. **538**, 689–698 (2019). https://doi.org/10.1016/j.jcis.2018.12.070
32. Sullivan, K.T., Wu, C., Piekiel, N.W., Gaskell, K., Zachariah, M.R.: Synthesis, and reactivity of nano-Ag2O as an oxidizer for energetic systems yielding antimicrobial products. Combust Flame. **160**, 438–446 (2013). https://doi.org/10.1016/j.combustflame.2012.09.011
33. Xiao, L., Youji, L., Feitai, C., Peng, X., Ming, L.: Facile synthesis of mesoporous titanium dioxide doped by Ag-coated graphene with enhanced visible-light photocatalytic performance for methylene blue degradation. RSC Adv. **7**, 25314–25324 (2017). https://doi.org/10.1039/c7ra02198d
34. Olya, M.E., Vafaee, M., Jahangiri, M.: Modeling of acid dye decolorization by TiO2–Ag2O nano-photocatalytic process using response surface methodology modeling of acid dye decolorization by TiO2–Ag2O nano-photocatalyts. J Saudi Chem Soc. **21**, 633–642 (2017). https://doi.org/10.1016/j.jscs.2015.07.006
35. Franco Jr., A., H.: V Pessoni, optical band-gap and dielectric behavior in Ho-doped ZnO nanoparticles. Mater Lett. **180**, 305–308 (2016)
36. Kumar, V., Singh, R.G., Purohit, L.P., Singh, F.: Effect of swift heavy ion on structural and optical properties of undoped and doped nanocrystalline zinc oxide films. Adv Mat Lett. **4**, 423–427 (2013)
37. Hosseini, M., Haghighatzadeh, A., Mazinani, B.: Enhanced third-order optical susceptibility in heterogeneous wurtzite ZnO/anatase TiO_2 core/shell nanostructures via controlled TiO2 shell thickness. Opt Mater (Amst). **92**, 1–10 (2019)